Photochemistry of (η^6-2,6-$X_2C_5H_3N$)$Cr(CO)_3$ (X = H, CH_3, $(CH_3)_3Si$). First Example of a Photoinduced Ring-Slip at an (η^6-Arene)$M(CO)_3$ Center. Molecular Structures of (η^6-2,6-$(CH_3)_2C_5H_3N$)$Cr(CO)_3$ and (η^6-2,6-$((CH_3)_3Si)_2C_5H_3N$)$Cr(CO)_3$

Ciara J. Breheny,[1a] Sylvia M. Draper,[1b] Friedrich-W. Grevels,[1c] Werner E. Klotzbücher,[1c] Conor Long,*[,1a] Mary T. Pryce,[1d] and Graham Russell*[,1c]

School of Chemical Sciences, Dublin City University, Dublin 9, Ireland, and Max-Planck-Institut für Strahlenchemie, Postfach 10 13 65, D-45413 Mülheim an der Ruhr, Germany

Received February 8, 1996[⊗]

The photochemistry of (η^6-2,6-$X_2C_5H_3N$)$Cr(CO)_3$ was investigated both in low-temperature matrices (X = H or $(CH_3)_3Si$) and in room-temperature solution (X = H, CH_3, or $(CH_3)_3$ Si). Room-temperature photolysis (λ_{exc} > 410 nm) in CO-saturated methanol or acetonitrile produced (η^1-2,6-$X_2C_5H_3N$)$Cr(CO)_5$ which subsequently formed $Cr(CO)_6$ in a secondary photochemical process (X = H or CH_3). The efficiency of pentacarbonyl formation is lower in CO-saturated cyclohexane and follows the order X = H > X = CH_3. Photolysis in low-temperature matrices resulted in an η^6 to η^1 pyridine ring-slippage (λ_{exc} = 460 nm; X = H). Visible irradiation in a CO-doped methane matrix produced (η^1-C_5H_5N)$Cr(CO)_5$, while in an N_2 matrix *fac*-(η^1-C_5H_5N)$(N_2)_2Cr(CO)_3$ is formed. Irradiation with λ_{exc} = 308 nm produced both the ring-slippage product and also the CO-loss product (η^6-C_5H_5)$Cr(CO)_2$, which in a N_2 matrix is trapped as (η^6- C_5H_5N)$Cr(CO)_2(N_2)$. Time-resolved infrared spectroscopy in cyclohexane revealed only the CO-loss product (λ_{exc} = 308 nm; X = H). The apparent difference in room-temperature and low-temperature photochemistry is explained by a rapid regeneration of (η^6-C_5H_5N)$Cr(CO)_3$ from the η^1-intermediate. This explanation was supported by laser flash photolysis experiments (λ_{exc} = 355 nm) in CO-saturated cyclohexane (Sol), where the recovery of the (η^6-C_5H_5N)$Cr(CO)_3$ absorption follows a biphasic time profile, whereby the faster process was assigned to the η^1 to η^6 transformation and the slower to the reaction of (η^6-C_5H_5N)$Cr(CO)_2$(Sol) with CO. Crystals of (η^6-2,6-$(CH_3)_2C_5H_3N$)$Cr(CO)_3$ and (η^6-2,6-$((CH_3)_3Si)_2C_5H_3N$)$Cr(CO)_3$ were characterized by X-ray diffraction.

Introduction

The chemistry of (η^6-arene)$M(CO)_3$ (M = Cr or Mo) has been the subject of numerous investigations, principally because of their use in both directing and promoting reactions at the arene ligand.[2] Also of interest have been the mechanisms of thermally induced ring exchange processes, which proceed *via* a stepwise ring displacement.[3] While arene exchange is also observed under photolytic conditions, the CO-loss product, (η^6-arene)$M(CO)_2$, has been implicated in this process (M = Cr).[4] To date, there are no reports in the literature of photoinduced haptotropic reactions for this class of compound.[5] It is accepted that CO loss is the dominant photoprocess in either low-temperature matrices,[6] room-temperature solution,[4] or the gas phase.[7] However, some indirect evidence for a second photoproduct, possibly one involving a haptotropic or ring-slip process, was obtained in our studies on the photochemistry of (η^6-C_6H_6)$Cr(CO)_3$.[8] Additional transient signals were observed following flash photolysis which could not be assigned to the known photoproduct (η^6-C_6H_6)$Cr(CO)_2$(solvent) or any species formed by a subsequent reaction of this intermediate. Consequently, we have investigated the photochemistry of a number of (η^6-arene)$M(CO)_3$ compounds in which the arene ligand contains a functionality designed to "trap" ring-slip intermediates, and the first results of these investigations are reported here.

⊗ Abstract published in *Advance ACS Abstracts,* August 1, 1996.

(1) (a) Dublin City University. (b) Present address: Department of Chemistry, University of Dublin, Trinity College, Dublin 2, Ireland. (c) The Max-Planck Institute. (d) Present address: Dipartimento di Chimica Organica e Industriale, Università degli Studi di Milano, via Golgi 19, 20133 Milano, Italy.

(2) *Transition metal organometallics for organic synthesis*; McQuillin, F. J., Parker, D. G., Stephenson, G. R., Eds.; Cambridge University Press: Cambridge, U.K., 1991.

(3) (a) Strohmeier, S.; Starrico, E. *Z. Phys. Chem. Neue Folge.* **1966**, *38*, 315. (b) Mahaffy, C. A. L.; Pauson,P. L. *J. Chem. Res. (S)* **1979**, 126. (c) Mahaffy, C. A. L.; Pauson, P. L. *J. Chem. Res. (M)* **1979**, 1752. (d) Zimmerman, C. L.; Shaner, J. L.; Royh, S. A.; Willeford, B. R. *J. Chem. Res. (S)* **1980**, 108. (e) Traylor, T. G.; Stewart, K. J.; Goldberg, M. J. *J. Am. Chem. Soc.* **1984**, *106*, 4445. (f) Traylor, T. G.; Stewart, K. J.; Goldberg, M. J. *Organometallics* **1986**, *5*, 2062. (g) Traylor, T. G.; Stewart, K. J. *J. Am. Chem. Soc.* **1986**, *108*, 6977. (h) Traylor, T. G.; Goldberg, M. J. *Organometallics* **1987**, *6*, 2413. (i) Traylor, T. G.; Goldberg, M. J. *Organometallics* **1987**, *6*, 2531.

(4) Gilbert, A.; Kelly, J. M.; Budzwait, M.; Koerner von Gustorf, E. *Z. Naturforsch.* **1976**, *31B*, 1091.

(5) Pryce, M. T. Ph.D. Thesis, Dublin City University, 1994.

(6) Rest, A. J.; Sodeau, J. R.; Taylor, D. J. *J. Chem. Soc., Dalton Trans.* **1978**, 651.

(7) Zheng, Y.; Wang, W.; Lin, J.; She, Y.; Fu, K.-J. *J. Phys. Chem.* **1992**, *96*, 9821.

(8) McGrath, I. M. Ph.D. Thesis, Dublin City University, 1993.

S0276-7333(96)00090-8 CCC: $12.00

Table 1. Summary of Crystal Data, Intensity Measurement, and Refinement for (η^6-2,6-$(CH_3)_2C_5H_3N$)$Cr(CO)_3$ and (η^6-2,6-$((CH_3)_3Si)_2C_5H_3N$)$Cr(CO)_3$

	compd	
	(η^6-$(CH_3)_2C_5H_3N$)$Cr(CO)_3$	(η^6-$((CH_3)_3Si)_2C_5H_3N$)$Cr(CO)_3$
formula	$C_{10}H_9NO_3Cr$	$C_{14}H_{21}NO_3CrSi_2$
cryst system	orthorhombic	monoclinic
space group	$Pna2_1$	$P2_1/n$
a, Å	13.0308(13)	7.7088(6)
b, Å	6.2875(6)	23.0928(9)
c, Å	12.7099(10)	10.4365(8)
β, deg		97.312(4)
V, Å^3	1041.3(2)	1842.8(2)
Z	4	4
d(calcd), g cm^{-3}	1.551	1.296
abs coeff, mm^{-1}	1.082	0.758
F(000)	496	752
cryst size, mm	0.5 × 0.5 × 0.25	0.4 × 0.4 × 0.3
θ range, deg	3.13−25.47	1.76−24.96
index ranges: h; k; l	0 to 13; −7 to 7; 0 to 14	0 to 8; 0 to 23; −11 to 11
reflcns collcd	1790	3326
indepdt reflcns	940 (R_{int} = 0.031)	3096 (R_{int} = 0.0177)
refinement method	full matrix on F^2	full-matrix on F^2
data/restraints/params	940/1/155	3096/0/203
goodness-of-fit on F^2	0.907	1.082
final R indices [$I > 2\sigma(I)$]	R_1 = 0.024; wR^2 = 0.060	$R1$ = 0.032; wR^2 = 0.078
R indices (all data)	R_1 = 0.055; wR^2 = 0.076	$R1$ = 0.074; wR^2 = 0.092
max diff peak, hole, e Å^{-3}	0.302, −0.253	0.308, −0.229

Heteroarenes, such as pyridine, constitute an ideal ligand type for these studies. These ligands offer the possibility of coordination *via* the ring π-electron system or, alternatively and more commonly, *via* the nitrogen atom. Furthermore the electronic spectra of all (η^6-arene)$Cr(CO)_3$ compounds are dominated by metal to ligand charge transfer transitions.[9] Both the HOMO and LUMO energies in pyridine are lower than the corresponding orbitals in benzene. Pyridine is therefore a poorer π-donor but a better π-acceptor ligand than benzene.[10] These differences may have significant consequences for the photochemistry of η^6-coordinated pyridine compounds. However, to our knowledge, there are no reports of such investigations. Consequently we have investigated the photochemistry of (η^6-C_5H_5N)$Cr(CO)_3$ and its 2,6-disubstituted derivatives by matrix isolation and time-resolved spectroscopic techniques in the hope of detecting haptotropic changes at the heteroarene ligand.

Structural determinations of (η^6-2,6-$(CH_3)_2C_5H_3N$)$Cr(CO)_3$ and (η^6-2,6-$((CH_3)_3Si)_2C_5H_3N$)$Cr(CO)_3$ were made to allow comparisons with the published molecular structure of (η^6-C_5H_5N)$Cr(CO)_3$.[11] In particular the effects of the bulky substituents in positions α to the nitrogen atom were of interest and also whether their presence could influence the subsequent thermal reactions following photochemical excitation.

Experimental Section

Synthesis of (η^6-C_5H_5N)$Cr(CO)_3$ and (η^6-2,6-$((CH_3)_3Si)_2C_5H_3N$)$Cr(CO)_3$. These complexes were synthesized by the method of Davies *et al.*[12] and were purified by recrystallization from diethyl ether/*n*-hexane mixtures. They were characterized by the standard spectroscopic and analytical techniques. In each case their purity was confirmed by both IR and NMR spectroscopy. Crystals of (η^6-2,6-$((CH_3)_3Si)_2C_5H_3N$)$Cr(CO)_3$ for structural analysis were grown from diethyl ether/*n*-hexane mixtures.

Synthesis of (η^6-$(CH_3)_2C_5H_3N$)$Cr(CO)_3$. $Cr(CO)_6$ (0.6 g) in 10 mL of dry THF was added to 50 mL of 2,6-$(CH_3)_2C_5H_3N$ and the solution brought to its reflux temperature for 8 h under a nitrogen atmosphere. The solution was then cooled to room temperature, and the solvent was removed under reduced pressure. The resulting yellow solid was purified by flash chromatography on neutral alumina (7:3 petroleum ether:diethyl ether (v/v) as the mobile phase). The identity and purity of this compound was confirmed by the standard range of spectroscopic and analytical techniques. Crystals for structural analysis were grown from diethyl ether/*n*-hexane mixtures.

Apparatus. Standard equipment included a Bruker AC400 NMR, a Perkin-Elmer 2000 FTIR, and a Hewlett Packard 8452A diode array UV/vis spectrophotometer. The matrix isolation apparatus has been described elsewhere,[13] including the devices for controlling the temperature (10−12 K), the flow of matrix gas (1.5−2 mmol h^{-1}), and metal complex deposition rate, the set-up for monochromatic and broad-band irradiation, and the IR and UV/vis spectrophotometers. The evaporation temperatures (30−35 °C) for (η^6-C_5H_5N)$Cr(CO)_3$ and (η^6-2,6-$((CH_3)_3Si)_2C_5H_3N$)$Cr(CO)_3$ were adjusted (quartz balance) to achieve a guest/host ratio ≤ 1/1000. The instrumentation for laser flash photolysis (308 nm, XeCl excimer laser, attenuated to 90−100 mJ/pulse) in combination with time-resolved IR detection (CaF_2 cell, d = 1 mm; globar IR source; HgCdTe detector; in the present configuration the system response is 1−2 μs), including the treatment of the sample solution, was recently described in detail[14] as was the UV/vis flash photolysis equipment.[15] Samples for the UV/vis monitored flash photolysis experiments were degassed by three cycles of freeze−pump−thaw to 10^{-3} Torr, followed by a substantial liquid pump to remove traces of water introduced in the degassing procedure. The samples were analyzed in a quartz cuvette

(9) Caroll, D. G.; McGlynn. S. P. *Inorg. Chem.* **1968**, *7*, 1285.
(10) Jorgenson, W. L.; Salem, L. *The Organic Chemists Book of Orbitals*; Academic Press: New York, 1973.
(11) Draper, S. M.; Byrne, J. J.; Breheny, C. J.; Long, C.; Low, J. N. *Acta Crystallogr.* **1994**, *C50*, 1669.
(12) Davies, S. G.; Shipton, M. R. *J. Chem. Soc., Perkin Trans. 1* **1991**, 501.
(13) (a) Gerhartz, W.; Grevels, F.-W.; Klotzbücher, W. E. *Organometallics* **1987**, *6*, 1850. (b) Klotzbücher, W. E. *Cryogenics* **1983**, *23*, 554.
(14) Grevels, F.-W.; Klotzbücher, W. E.; Schrickel, J.; Schaffner, K. *J. Am. Chem. Soc.* **1994**, *116*, 6229.
(15) Creaven, B. S.; George, M. W.; Ginzburg, A. G.; Hughes, C.; Kelly, J. M.; Long, C.; McGrath, I. M.; Pryce, M. T. *Organometallics* **1993**, *12*, 3127.

Table 2. Spectroscopic Data for the Compounds in This Investigation

compd	λ_{max} (ϵ)[a]	ν_{CO} (cm^{-1})[b]	^1H NMR[c]
$Cr(CO)_6$	280	1986[d]	
(η^6-C_5H_5N)$Cr(CO)_3$	316 (8.36 × 10^3)	1997, 1939, 1926[d]	6.55 (m, 2H), 5.65 (m, 1H), 5.23 (m, 2H)
(η^6-C_5H_5N)$Cr(CO)_3$[e]		2000, 1942, 1926	
(η^6-C_5H_5N)$Cr(CO)_3$[f]		1996, 1935, 1920	
(η^6-C_5H_5N)$Cr(CO)_3$[g]		1999, 1938, 1924	
(η^1-C_5H_5N)$Cr(CO)_3$[g]		1957, 1841, 1833	
(η^1-C_5H_5N)$Cr(CO)_3$[h]		1956, 1841, 1833	
(η^6-C_5H_5N)$Cr(CO)_2$(Sol)[d]		1950, 1890	
(η^6-C_5H_5N)$Cr(CO)_2$[g]		1945, 1888	
(η^6-C_5H_5N)$Cr(CO)_2(N_2)$[e]		1957, 1910	
fac-(η^1-C_5H_5N)$(N_2)_2Cr(CO)_3$[e]		1967, 1897, 1885	
(η^1-C_5H_5N)$Cr(CO)_4$[h]		2030, 1909, 1907, 1870	
(η^1-C_5H_5N)$Cr(CO)_5$	410	2068, 1938, 1919[d]	8.5 (d, 2H), 7.7 (t, 1H), 7.3 (m, 2H)
(η^1-C_5H_5N)$Cr(CO)_5$[f]		2070, 1938, 1914	
(η^6-2,6-$(CH_3)_2C_5H_3N$)$Cr(CO)_3$	318 (6.07 × 10^3)	1987, 1926, 1917[d]	5.65 (t, 1H), 5.12 (d, 2H), 2.41 (s, 6H)
(η^6-2,6-$((CH_3)_3$ Si)$_2C_5H_3N$)$Cr(CO)_3$	324 (7.69 × 10^3)	1978, 1912 (br)[d]	5.48 (d, 2H), 5.29 (t, 1H), 0.3 (s, 18H)
(η^6-2,6-$((CH_3)_3$ Si)$_2C_5H_3N$)$Cr(CO)_3$[f]		1986, 1923, 1918	
(η^6-2,6-$((CH_3)_3$ Si)$_2C_5H_3N$)$Cr(CO)_3$[e]		1988, 1926, 1919	
(η^6-2,6-$((CH_3)_3$ Si)$_2C_5H_3N$)$Cr(CO)_2$[f]		1942, 1890	
(η^6-2,6-$((CH_3)_3$Si)$_2C_5H_3N$)$Cr(CO)_2(N_2)$[e]		1947, 1907	
(η^1-2,6-$((CH_3)_3$Si)$_2C_5H_3N$)$Cr(CO)_3$[f]		1954, 1854, 1848	

[a] nm in cyclohexane solution ± 2 nm (±1% L mol^{-1} cm^{-1}). [b] ± 1 cm^{-1}. [c] ppm in $CDCl_3$ at 400 MHz. [d] In cyclohexane solution at 298 K. [e] In an N_2 matrix at 12 K. [f] 10% CO in Ar matrix at 12 K. [g] In a CH_4 matrix at 10 K. [h] 10% CO in CH_4 matrix at 12 K.

with four optical flat walls. The excitation and monitoring beams were arranged in a cross-beam configuration.

Single-Crystal Structural Determinations. X-ray diffraction data were collected on an Enraf-Nonius CAD4 automatic diffractometer at room temperature. The structures were solved using the Patterson strategy of Shelxs-86[16] and refined by full-matrix least squares on F^2 using Shelxl-93.[17] Manipulations of the molecular structures were made using Schakal-92.[18] The crystal, intensity, and refinement data are presented in Table 1.

Results

The spectroscopic details of the compounds in this investigation are given in Table 2, and the UV/vis spectrum of (η^6-C_5H_5N)$Cr(CO)_3$ in cyclohexane solution is given in Figure 1a. The compound shows the characteristic absorptions of (η^6-arene)$Cr(CO)_3$ compounds with λ_{max} at approximately 320 nm. Unfortunately, the valley in the absorption profile at 290 nm is not as pronounced in this compound as in the (η^6-C_6H_6)$Cr(CO)_3$ analogue. This valley has been used as a window into the UV region for the detection of transient species which have little or no absorptions in the visible region of the spectrum. The infrared spectrum of (η^6- C_5H_5N)-$Cr(CO)_3$ in the ν_{C-O} region is presented in Figure 1b. Three absorptions of almost equal intensity are observed for this compound which has C_s symmetry. This makes the interpretation of the matrix isolation and TRIR results both simple and unambiguous. The number of ν_{C-O} absorption bands will equal the number of carbonyl ligands in a particular photofragment.

Steady-State Photolysis of (η^6-2,6-$X_2C_5H_3N$)Cr-$(CO)_3$. The photochemistry of (η^6-2,6-$X_2C_5H_3N$)$Cr(CO)_3$ was investigated in either CO-saturated acetonitrile, methanol, or cyclohexane and followed by ^1H NMR or UV/vis spectroscopy (λ_{exc} > 410 nm). The NMR changes in the aromatic region observed in CD_3CN for X = H

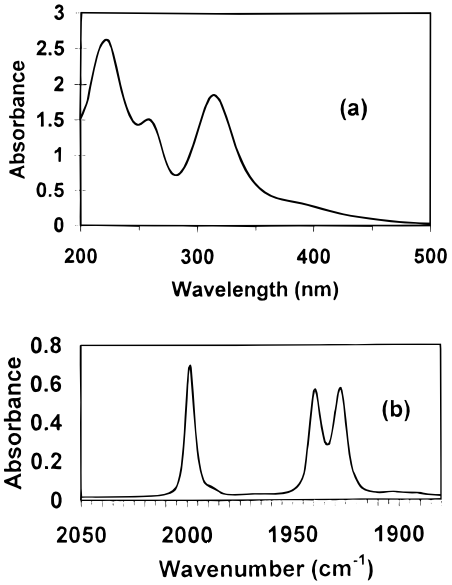

Figure 1. (a) UV/vis spectrum of (η^6-C_5H_5N)$Cr(CO)_3$ (2 × 10^{-4} M) in cyclohexane and (b) its infrared spectrum in the ν_{C-O} region also in cyclohexane solution.

are presented in Figure 2 and indicate a reduction in the intensity of the bands of the parent, with concomitant formation of bands assigned to (η^1-C_5H_5N)$Cr(CO)_5$. This was confirmed by comparison of the final spectrum with that of an authentic sample of (η^1-C_5H_5N)$Cr(CO)_5$ prepared independently. The relative quantum efficiency for the disappearance of (η^6-2,6-$X_2C_5H_3N$)Cr-$(CO)_3$ depends on the solvent and the substituent X as measured by UV/vis spectroscopy (λ_{exc} > 410 nm). The reduction in the absorbance of the η^6 species was measured for photochemical conversions of <15% to minimize internal light filter effects by the product. The results were normalized to account for minor variations in the absorbance between the particular solutions. The

(16) Sheldrick, G. M. SHELXS-86, Programme for Crystal Structure Determination. *Acta Crystallogr.* **1990**, *A46*, 467.

(17) Sheldrick, G. M. SHELXL-93, Programme for Crystal Structure Refinement, University of Göttingen, Göttingen, Germany, 1993.

(18) Keller, E. SCHAKAL-92, A Programme for Graphical representation of Molecular Structures, Kristallographisches Institut der Universitaet, Freiburg, Germany, 1992.

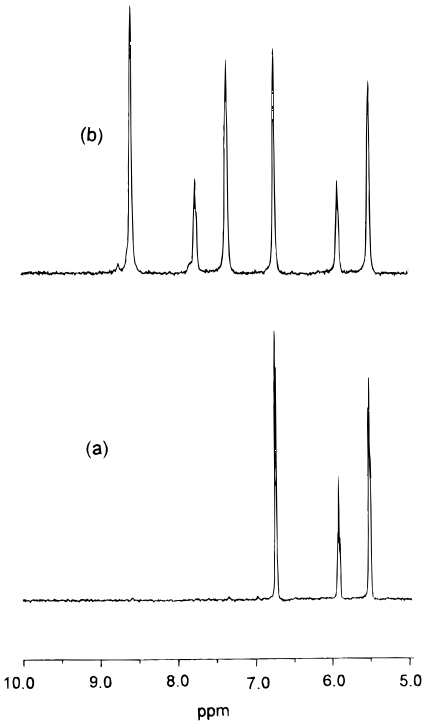

Figure 2. ^{1}H NMR spectral changes in the aromatic region observed following photolysis (λ_{exc} > 410 nm; 275 W Xe-arc lamp) of (η^6-C_5H_5N)$Cr(CO)_3$ in CO-saturated CD_3CN (at 400 MHz). Spectrum a represents the initial spectrum. Spectrum b was obtained following 55 min of irradiation indicating the formation of the (η^1-C_5H_5N)$Cr(CO)_5$ as verified by comparison with the spectrum of (η^1-C_5H_5N)-$Cr(CO)_5$ synthesized by an independent route.

Scheme 1

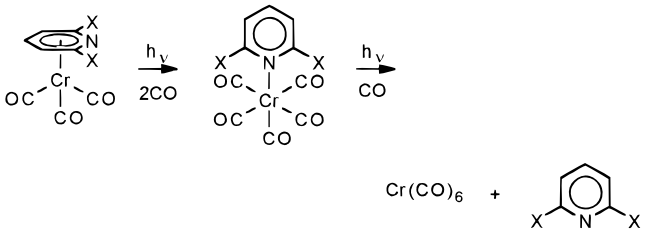

process is 2.5 times more efficient in CH_3OH than C_6H_{12} and 2.3 times more efficient for X = H than for X = CH_3 in cyclohexane. For X = $(CH_3)_3Si$ the efficiency is essentially zero in cyclohexane. In this latter solvent the (η^1-C_5H_5N)$Cr(CO)_5$ produced subsequently undergoes further photochemical loss of the pyridine ligand producing $Cr(CO)_6$ (confirmed by ^{13}C NMR). The overall reaction sequence is outlined in Scheme 1.

Matrix Isolation Photochemistry of (η^6-C_5H_5N)-$Cr(CO)_3$. The photochemistry of (η^6-C_5H_5N)$Cr(CO)_3$ was investigated in a methane matrix at 10 K. With long-wavelength irradiation (λ_{exc} = 460 nm) the bands of the parent species at 1999, 1938, and 1924 cm^{-1} were depleted with concomitant formation of three bands at 1957, 1841, and 1833 cm^{-1} (Figure 3a), indicative of a *fac*-$Cr(CO)_3$ moiety. These bands were assigned to a heteroarene ring-slip product of the type (η^x-C_5H_5N)-$Cr(CO)_3$ (x < 6). Irradiation at shorter wavelength (λ_{exc} = 308 nm) yields the same species but in addition produces further bands at 1945 and 1888 cm^{-1} (the latter band is subject to matrix splitting, Figure 3b) along with a weak feature at 2136 cm^{-1} attributable to free CO. The frequency separation of 57 cm^{-1} in the

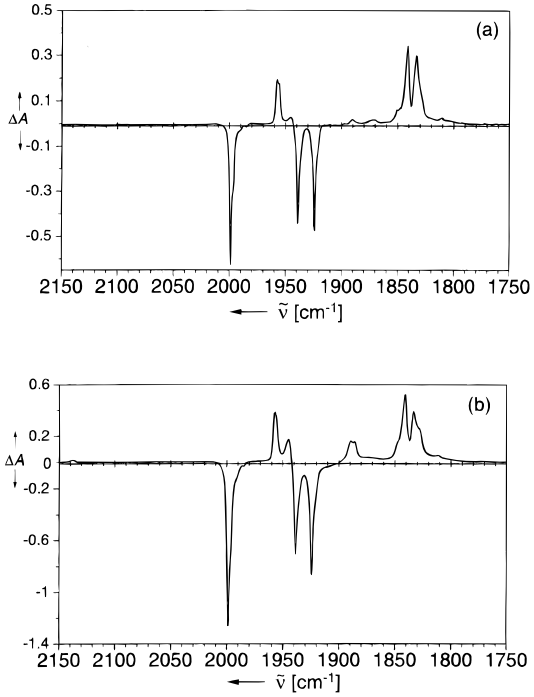

Figure 3. (a) Difference spectrum obtained following irradiation (λ_{exc} = 460 nm) of a CH_4 matrix containing (η^6-C_5H_5N)$Cr(CO)_3$ at 10 K and (b) spectrum obtained in a separate experiment following irradiation with λ_{exc} = 308 nm (negative peaks indicate depletion of the parent compound).

new two-band pattern compares with that observed for (η^6-C_6H_6)$Cr(CO)_2$ (55 cm^{-1}), photogenerated from (η^6-C_6H_6)$Cr(CO)_3$ in a methane matrix,[6] thereby suggesting the assignment as the CO-loss product (η^6-C_5H_5N)Cr-$(CO)_2$ (reaction 1). Further support for this assignment

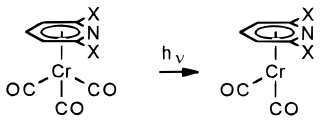

(1)

comes from a comparison of the frequency shifts in going from the respective parent tricarbonyl complexes to (η^6-C_6H_6)$Cr(CO)_2$ (56 and 43 cm^{-1})[6] and (η^6-C_5H_5N)$Cr(CO)_2$ (54 and 43 cm^{-1}); in the latter case the average wavenumber of the two low-energy bands of the parent complex (1931 cm^{-1}) was taken.

To determine the degree to which the hapticity of the pyridine−chromium interaction has been changed following long-wavelength irradiation, experiments were conducted in both an N_2- and a CO-doped methane matrix. Irradiation in an N_2 matrix (λ_{exc} = 460 nm) produced three bands (1967, 1897, and 1885 cm^{-1}) along with two absorptions of comparable intensities in the ν_{N-N} region (2222 and 2189 cm^{-1}) as presented in Figure 4a. This pattern is indicative of a facial arrangement of three CO groups and two *cis*-coordinated N_2 ligands,[19] which logically implies an η^1 coordination of the pyridine

(19) The wavenumber difference between the ν_{N-N} antisymmetric and symmetric vibrational modes of 33 cm^{-1} is similar to the 39 cm^{-1} difference observed in (η^5-C_5H_5)$Nb(CO)_2(N_2)_2$: George, M. W.; Haward, M. T.; Hamley, P. A.; Hughes, C.; Johnson, F. P. A.; Popov, V. K.; Poliakoff, M. *J. Am. Chem. Soc.* **1993**, *115*, 2286.

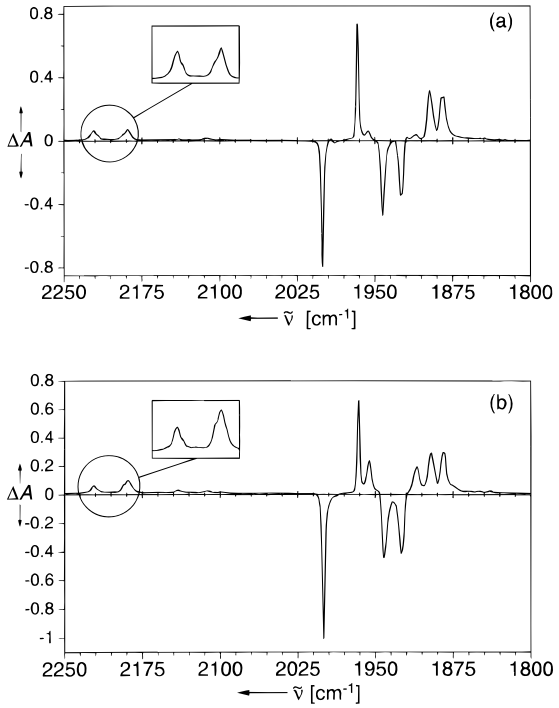

Figure 4. (a) Difference spectrum obtained following photolysis of (η^6-C_5H_5N)Cr(CO)$_3$ in an N_2 matrix (λ_{exc} = 460 nm) showing the two bands in the ν_{N-N} region at 2221 and 2188 cm^{-1} (cf. inset) assigned to *fac*-(η^1-C_5H_5N)(N_2)$_2$Cr(CO)$_3$ and (b) spectral changes obtained following irradiation with λ_{exc} = 308 nm with the inset showing the ν_{N-N} bands for the N_2 adducts of both ring-slip and CO-loss species.

ligand (reaction 2). Irradiation of a similar matrix with

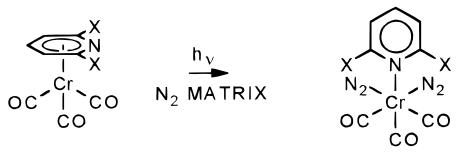

(2)

λ_{exc} = 308 nm produced additional ν_{C-O} bands at 1957 and 1910 cm^{-1} (Figure 4b) while in this case the bands observed in the ν_{N-N} region have significantly different relative intensities (cf. insets in Figure 4). A weak feature attributable to free CO (2140 cm^{-1}) is also observed in this experiment. These observations can be explained by the simultaneous formation of the ring-slip and the CO-loss product both of which in turn take up N_2 from the environment producing (η^1-C_5H_5N)Cr(CO)$_3$(N_2)$_2$ and (η^6-C_5H_5N)Cr(CO)$_2$(N_2), respectively. The ν_{N-N} band of the latter species overlaps the low-energy ν_{N-N} band of the bis(dinitrogen) species at 2189 cm^{-1}.

Photolysis of (η^6-C_5H_5N)Cr(CO)$_3$ in a CH_4:CO matrix (10:1) (λ_{exc} = 460 nm) produced a three-band pattern (2070, 1937, and 1916 cm^{-1}) characteristic of (η^1-C_5H_5N)Cr(CO)$_5$ (Figure 5),[20] thus indicating a photoinduced η^6 to η^1 haptotropic shift, followed by the takeup of two CO ligands from the matrix. An additional band at 1983 cm^{-1} assigned to Cr(CO)$_6$ was also observed. Subsequent photolysis with λ_{exc} = 250 nm produced peaks at 2031, 1909, 1907, and 1870 cm^{-1}, which have been assigned to the (η^1-C_5H_5N)Cr(CO)$_4$ species with a vacant site *cis* to the pyridine ligand, produced from (η^1-C_5H_5N)Cr(CO)$_5$. Photolytic loss of CO from the tetracarbonyl fragment yields (η^1-C_5H_5N)Cr(CO)$_3$ (1956, 1841, and 1831 cm^{-1}), which is identified by comparison with the data obtained in a methane matrix (cf. Table 2), for (η^1-C_5H_5N)Cr(CO)$_3$ generated from (η^6-C_5H_5N)Cr(CO)$_3$. Subsequent long-wavelength photolysis (λ_{exc} > 530 nm) regenerated (η^1-C_5H_5N)Cr(CO)$_5$ at the expense of both (η^1-C_5H_5N)Cr(CO)$_3$ and (η^1-C_5H_5N)Cr(CO)$_4$. Further irradiation with λ_{exc} = 400 nm produced Cr(CO)$_6$ (1984 cm^{-1}), which dominates the spectrum as the ultimate product of the overall reaction sequence, and a band at 1958 cm^{-1} the assignment of which is uncertain but could be either the ^{13}C satellite of Cr(CO)$_6$ or possibly one of the bands of Cr(CO)$_5$(CH_4).[21]

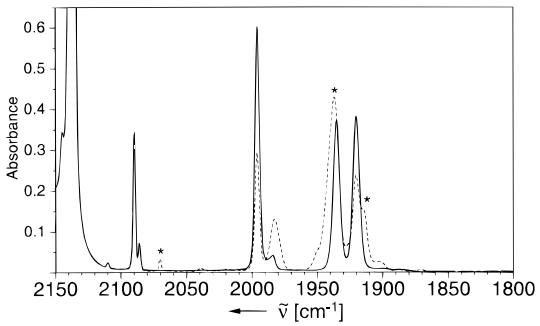

Figure 5. Infrared spectra recorded before (—) and after (- - -) irradiation (λ_{exc} = 460 nm; 60 min) of (η^6-C_5H_5N)Cr(CO)$_3$ in a CH_4:CO matrix (10:1) showing the formation of (η^1-C_5H_5N)Cr(CO)$_5$ (marked *) and Cr(CO)$_6$ (1983 cm^{-1}). The absorptions above 2080 cm^{-1} originate from the carbon monoxide in the matrix.

Matrix Photochemistry of (η^6-2,6-((CH$_3$)$_3$Si)$_2$-C_5H_3N)Cr(CO)$_3$. Photolysis (λ_{exc} = 460 nm) of (η^6-2,6-((CH$_3$)$_3$Si)$_2$$C_5H_3N$)Cr(CO)$_3$ in an Ar matrix containing 10% CO failed to cause any significant IR spectral changes. However photolysis with λ_{exc} = 250 nm resulted in a depletion of the parent bands and the appearance of new bands at 1942 and 1890 cm^{-1} assigned to the CO-loss product (η^6-2,6-((CH$_3$)$_3$Si)$_2$-C_5H_3N)Cr(CO)$_2$. Subsequent irradiation at 308 nm lead to a further increase of the bands of the dicarbonyl species but also produced bands at 1954, 1854, and 1848 cm^{-1}, which, by comparison with the photochemistry of (η^6-C_5H_5N)Cr(CO)$_3$ in CH_4 matrices, are assigned to (η^1-2,6-((CH$_3$)$_3$Si)$_2$$C_5H_3N$)Cr(CO)$_3$. White light photolysis results in a depletion of all product bands and the reformation of the parent tricarbonyl compound, thus illustrating an efficient photoreversal of both the CO-loss and η^1-species.

In an N_2 matrix, irradiation of (η^6-2,6-((CH$_3$)$_3$Si)$_2$-C_5H_3N)Cr(CO)$_3$ with λ_{exc} = 460 nm resulted in the depletion of the parent bands with concomitant liberation of CO (2140 cm^{-1}) and formation of (η^6-2,6-((CH$_3$)$_3$-Si)$_2$$C_5H_3N$)Cr(CO)$_2$($N_2$) ($\nu_{C-O}$ 1947 and 1907 cm^{-1}; ν_{N-N} = 2180 cm^{-1}) albeit with low efficiency. This observation demonstrates that at this wavelength of excitation the complex is not entirely photochemically inert, as might be concluded from the experiment in the CO-doped Ar matrix. On the basis of some additional weak features in the ν_{C-O} region, one might conclude that the η^6 to η^1 ring-slippage also takes place, but it was impossible to determine if this species interacts with the N_2 from the matrix environment because of the weakness of the bands.

(20) Braterman, P. S. *Metal Carbonyl Spectra*; Academic Press: New York, 1975.

(21) Perutz, R. N.; Turner, J. J. *J. Am. Chem. Soc.* **1975**, *75*, 4791.

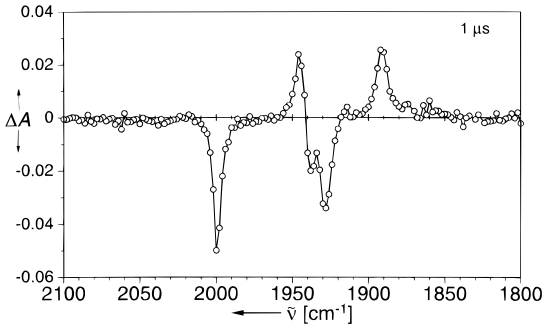

Figure 6. TRIR difference spectrum in cyclohexane at room temperature obtained 1 μs after the laser pulse (λ_{exc} = 308 nm) of (η^6-C_5H_5N)$Cr(CO)_3$ (5×10^{-4} M), showing depletion of the parent compound and the formation of (η^6-C_5H_5N)$Cr(CO)_2$(cyclohexane).

Time-Resolved Infrared Spectroscopy. Laser flash photolysis of (η^6-C_5H_5N)$Cr(CO)_3$ was monitored by TRIR spectroscopy at room temperature in CO-saturated cyclohexane solution ([CO] = 9.0×10^{-3} M).[22] Figure 6 represents the difference spectrum obtained 1 μs after the laser pulse (λ_{exc} = 308 nm). The negative peaks at 1999, 1940, and 1930 cm^{-1} correspond to depletion of the parent absorptions, while the product bands at 1950 and 1890 cm^{-1} are close to those obtained for (η^6-C_5H_5N)$Cr(CO)_2$ in the CH_4 matrix experiments (Table 2) and were assigned to (η^6-C_5H_5N)$Cr(CO)_2$(Sol) (Sol = cyclohexane). These bands decay by first-order kinetics ($k_{obs} = 2.1 \times 10^5$ s^{-1}) with partial regeneration of the starting material (reaction 3).

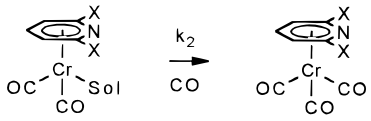

(3)

At first sight, loss of CO with formation of the species (η^6-C_5H_5N)$Cr(CO)_2$(Sol) seems to be the only process observable by time-resolved IR spectroscopy. However, on closer inspection it is apparent that some (η^1-C_5H_5N)-$Cr(CO)_5$ is also detectable, as observed in steady-state photolyses in CO-saturated solution (Scheme 1). Unfortunately, the high-frequency A_1 vibration of (η^1-C_5H_5N)$Cr(CO)_5$ at approximately 2070 cm^{-1} is inherently weak (cf. Figure 5), which makes this feature difficult to detect in the time-resolved experiments. Moreover, the low-frequency A_1 and the E stretching vibrations are almost coincidental with the low-frequency bands of the parent tricarbonyl (Figure 5; see Table 2). The spectral changes accompanying the partial recovery of the parent ultimately lead to a difference spectrum showing positive absorptions at 1948, 1920, and 1880 cm^{-1}. The former pair represent the E and A_1 modes of (η^1-C_5H_5N)$Cr(CO)_5$ mentioned above, while the latter feature remains unidentified, a dinuclear species being a plausible candidate.

Flash Photolysis with UV/Vis Detection. The photochemistry of (η^6-2,6-$X_2C_5H_3N$)$Cr(CO)_3$ (X = H, CH_3, or $(CH_3)_3Si$) was investigated by UV/vis flash photolysis with λ_{exc} = 355 nm in CO-saturated cyclohexane. The difference spectrum obtained 5 μs after the laser pulse is given in Figure 7 for X = H. From this spectrum it can be seen that the only region of the spectrum where the photoproducts absorb significantly is in the valley at 290 nm of the parent absorption spectrum and a weak feature at approximately 500 nm. Analysis of the decay kinetics associated with the transient absorption at 280 nm (Table 3) yields the rate constant for the reaction with CO (k_2; reaction 3). The transient signal at this wavelength indicates that the system is not fully reversible. This absorption is assigned to the CO-loss product. Under these conditions, the parent absorption (monitored at 340 nm) recovers by two temporally resolved processes. The slower process, i.e., that occurring after the time indicated by the arrow in the inset in Figure 7, corresponds to the re-formation of (η^6-2,6-$X_2C_5H_3N$)$Cr(CO)_3$ species *via* the reaction of (η^6-2,6-$X_2C_5H_3N$)$Cr(CO)_2$(Sol) with CO. The faster process is complete at the time indicated by the arrow. The terminal impedence was reduced in efforts to measure this signal accurately, but it appears to be completed within a time scale too close to the theoretical rise-time of the equipment (~40 ns) for it to be reliably measured and corresponds to the recovery of (η^6-2,6-$X_2C_5H_3N$)$Cr(CO)_3$ from the (η^1-2,6-$X_2C_5H_3N$)$Cr(CO)_3$ intermediate.

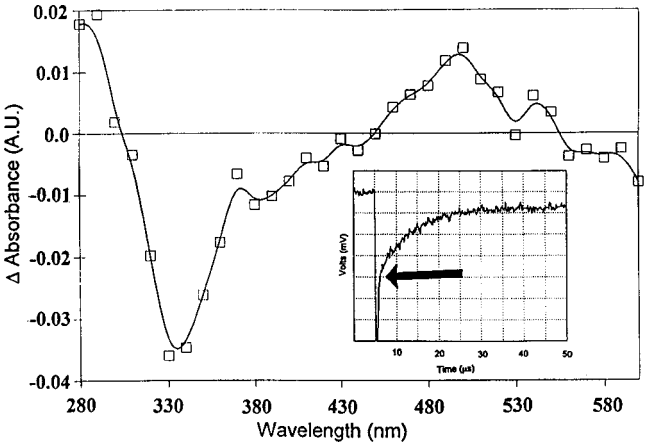

Figure 7. UV/vis difference spectrum obtained following 5 μs after photolyis (λ_{exc} = 355 nm) of (η^6-C_5H_5N)$Cr(CO)_3$ in CO-saturated cyclohexane at room temperature. The inset shows the transient signal at 340 nm indicating that two temporally resolved processes are associated with the recovery of the parent absorption. The first process, completed by the time indicated by the arrow, is assigned to the η^1 to η^6 haptotropic reversal, while the second process corresponds to the reaction of the CO-loss species with CO.

Table 3. Second-Order Rate Constants (k_2) for the Reaction of (η^6-2,6-$X_2C_5H_3N$)$Cr(CO)_2$(Sol) with CO at 298 K

X	k_2[a]	technique	X	k_2[a]	technique
H	1.4	TRIR	CH_3	1.5	UV flash photolysis
H	1.4	UV flash photolysis	$(CH_3)_3Si$	2	UV flash photolysis

[a] $\times 10^{-7}$ (±10%) M^{-1} s^{-1} in cyclohexane solution.

Crystal and Molecular Structures of (η^6-2,6-$(CH_3)_2C_5H_3N$)$Cr(CO)_3$ and (η^6-2,6-$((CH_3)_3Si)_2C_5H_3N$)-$Cr(CO)_3$. Both molecules consist of a heteroarene ring to which a chromium tricarbonyl unit is coordinated *via* its ring π-system (Figure 8). The chromium atom is located directly below the arene ring centroid, and the arene ring is essentially planar. In the case of the 2,6-$(CH_3)_2C_5H_3N$ compound the carbonyl ligands eclipse the 2, 4, and 6 arene carbons; thus carbonyl C10−O2 is *trans* to the ring nitrogen. This conformation is also observed in the unsubstituted (η^6-C_5H_5N)$Cr(CO)_3$ com-

(22) Makrancszy, J.; Megyery-Balog, K.; Rosz, L.; Patyt, D. *Hung. J. Indust. Chem.* **1976**, *4*, 269.

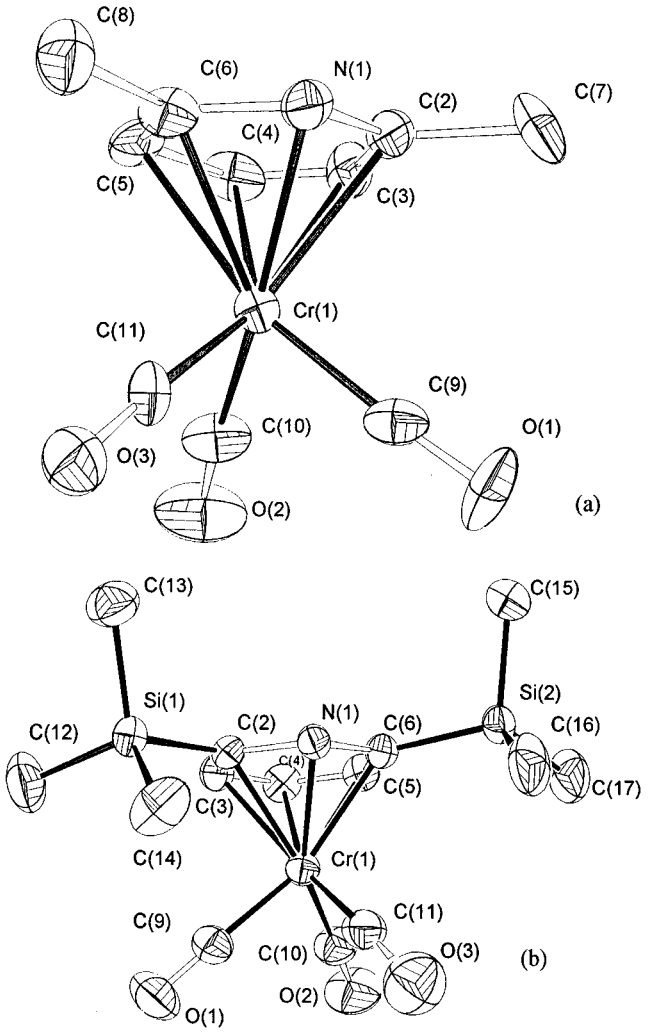

Figure 8. ORTEP diagrams of the molecular structures of (a) (η^6-2,6-$(CH_3)_2C_5H_3N$)Cr(CO)$_3$ and (b) (η^6-2,6-$((CH_3)_3Si)_2C_5H_3N$)Cr(CO)$_3$ showing the atom numbering system used (hydrogen atoms are omitted for clarity).

pound previously published.[11] In the (η^6-2,6-$((CH_3)_3Si)_2C_5H_3N$)Cr(CO)$_3$ compound the carbonyl groups are in a staggered conformation and eclipse the ring bond centers. This conformation appears to have little effect on the Cr−ring-centroid distance which is identical in the trimethylsilyl compound (1.698(3) Å) to that of the unsubstituted pyridine compound (1.697(4) Å).[11] Table 4 contains a selected listing of bond lengths and angles for both compounds.

Discussion

The formation of (η^1-C_5H_5N)Cr(CO)$_5$ and ultimately Cr(CO)$_6$ in the presence of CO demonstrates that CO loss is not the only photochemical route accessible to (η^6-C_5H_5N)Cr(CO)$_3$. The efficiency of formation of the pentacarbonyl species in solution depends on the nature of the solvent and also the substituents on the 2,6-positions. Consequently (η^1-2,6,-$X_2C_5H_3N$)Cr(CO)$_5$ is formed most efficiently in methanol for X = H. These studies indicate that formation of (η^1-2,6-$X_2C_5H_3N$)Cr(CO)$_5$ requires the initial formation of an intermediate species, whose stability is influenced by the Lewis base character of the solvent and/or the size of the substituents α to the nitrogen atom. The matrix isolation experiments allow us to propose a model for this intermediate species.

Table 4. Selected Bond Lengths (Å) and Angles (deg) with Esd's in Parentheses for (η^6-2,6-$((CH_3)_3Si)_2C_5H_3$)Cr(CO)$_3$ and (η^6-2,6-$(CH_3)_2C_5H_3N$)Cr(CO)$_3$

	(η^6-2,6-$((CH_3)_3Si)_2$-C_5H_3)Cr(CO)$_3$	(η^6-$(CH_3)_2C_5H_3N$)-Cr(CO)$_3$
Cr(1)−C(9)	1.835(3)	1.86(2)
Cr(1)−C(10)	1.846(3)	1.847(5)
Cr(1)−C(11)	1.846(3)	1.82(2)
Cr(1)−N(1)	2.180(2)	2.220(4)
Cr(1)−C(2)	2.183(3)	2.21(2)
Cr(1)−C(5)	2.198(3)	2.26(2)
Cr(1)−C(6)	2.205(3)	2.191(14)
Cr(1)−C(3)	2.204(3)	2.22(2)
Cr(1)−C(4)	2.209(3)	2.242(5)
C(9)−Cr(1)−C(10)	86.44(14)	87.6(8)
C(9)−Cr(1)−C(11)	85.44(14)	84.8(2)
C(10)−Cr(1)−C(11)	89.1(2)	89.3(8)
C(9)−Cr(1)−N(1)	118.98(11)	101.8(6)
C(10)−Cr(1)−N(1)	154.56(12)	166.1(2)
C(11)−Cr(1)−N(1)	91.83(12)	101.6(7)
C(9)−Cr(1)−C(2)	93.14(12)	90.8(7)
C(10)−Cr(1)−C(2)	153.91(13)	136.1(8)
C(11)−Cr(1)−C(2)	116.90(13)	134.3(7)
N(1)−Cr(1)−C(2)	36.53(8)	35.2(6)
C(9)−Cr(1)−C(5)	154.24(13)	165.7(7)
C(10)−Cr(1)−C(5)	90.57(13)	103.6(7)
C(11)−Cr(1)−C(5)	120.12(13)	104.0(7)
N(1)−Cr(1)−C(5)	67.11(10)	65.6(5)
C(2)−Cr(1)−C(5)	78.58(11)	74.9(5)
C(9)−Cr(1)−C(6)	156.13(12)	133.6(6)
C(10)−Cr(1)−C(6)	117.41(13)	138.3(8)
C(11)−Cr(1)−C(6)	93.47(12)	88.4(7)
N(1)−Cr(1)−C(6)	37.16(9)	35.3(6)
C(2)−Cr(1)−C(6)	66.09(10)	62.6(2)
C(5)−Cr(1)−C(6)	37.09(10)	37.5(6)
C(9)−Cr(1)−C(3)	92.64(13)	105.9(6)
C(10)−Cr(1)−C(3)	116.26(14)	103.3(7)
C(11)−Cr(1)−C(3)	154.44(13)	163.6(7)
N(1)−Cr(1)−C(3)	66.85(10)	64. 5(6)
C(2)−Cr(1)−C(3)	37.66(10)	35.7(7)
C(5)−Cr(1)−C(3)	65.88(12)	63.2(2)
C(6)−Cr(1)−C(3)	78.15(11)	75.2(6)
C(9)−Cr(1)−C(4)	117.15(13)	136.6(8)
C(10)−Cr(1)−C(4)	89.75(14)	88.6(2)
C(11)−Cr(1)−C(4)	157.25(13)	138.3(8)
N(1)−Cr(1)−C(4)	79.74(10)	77.5(2)
C(2)−Cr(1)−C(4)	67.26(11)	35.2(6)
C(5)−Cr(1)−C(4)	37.17(11)	37.1(8)
C(6)−Cr(1)−C(4)	67.09(11)	66.7(5)
C(3)−Cr(1)−C(4)	36.51(11)	34.1(8)

The photochemistry of (η^6-C_5H_5N)Cr(CO)$_3$ in a range of isolating matrices exhibited a wavelength dependency. Irradiation with λ_{exc} = 460 nm results in the formation of a *fac*-Cr(CO)$_3$ unit which in a N_2 matrix yields a *fac*-Cr(CO)$_3$(N_2)$_2$ fragment. These results are consistent with an η^6 to η^1 haptotropic shift, thus generating two vacant sites on the metal. In a CO-doped matrix this species can capture two CO ligands to produce (η^1-C_5H_5N)Cr(CO)$_5$, while in a N_2 matrix *fac*-(η^1-C_5H_5N)Cr(CO)$_3$(N_2)$_2$ is formed.

The matrix photochemistry of (η^6-2,6-$((CH_3)_3Si)_2$-C_5H_3N)Cr(CO)$_3$ proved to be interesting. Even though experiments were conducted in a CO-doped matrix, no evidence for the formation of pentacarbonyl or hexacarbonyl species was obtained. In this respect the matrix results are comparable to those obtained for this compound in room-temperature solution. The products formed upon short-wavelength photolysis are sensitive to photoreversal with white light. Hence, the failure to observe any photochemistry following irradiation at λ_{exc} = 460 nm in this medium may simply reflect an

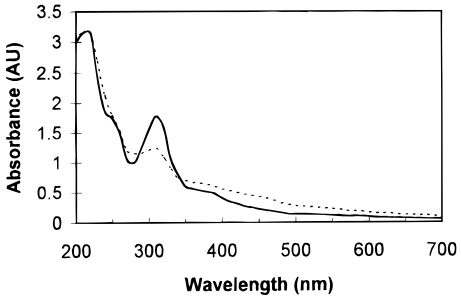

Figure 9. The UV/vis spectrum of (η^6-C_5H_5N)$Cr(CO)_3$ in a CH_4 matrix at 12 K (—) and the same matrix following irradiation for 60 s with λ_{exc} = 308 nm (- - -). These spectra are not corrected for matrix scatter.

efficient photoreversal of the initial product. Figure 9 confirms that photolysis of (η^6-C_5H_5N)$Cr(CO)_3$ (λ_{exc} = 308 nm) in a methane matrix, producing both the CO-loss and ring-slip products, exhibits an unstructured absorption well into the visible region of the spectrum. The photochemistry of (η^6-2,6-$((CH_3)_3Si)_2C_5H_3N$)$Cr(CO)_3$ in an N_2 matrix is dominated by a low-efficiency CO loss even following long-wavelength irradiation. Some evidence for the formation of an η^1-species is observed, but no ν_{N-N} bands associated with this species could be detected. Therefore it is not possible to confirm if this ring-slip species interacts with the N_2 matrix to any significant degree.

The lack of any evidence for CO or N_2 addition to the (η^1-2,6-$((CH_3)_3Si)_2C_5H_3N$)$Cr(CO)_3$ species can be explained in terms of the steric crowding in the coordination sphere of the chromium atom. The structural parameters obtained from the X-ray data provide an estimate of the steric requirements of the 2,6-$((CH_3)_3Si)_2C_5H_3N$ ligand. Using the "Unlock Model" facility in Schakal-92,[18] the chromium tricarbonyl unit was located 2.0 Å from the nitrogen atom. This is approximately where it would be following an η^6 to η^1 haptotropic shift. Analysis of the close contacts for this orientation indicated that there is sufficient freedom to permit coordination of the pyridine nitrogen atom to the chromium tricarbonyl unit but not to higher order carbonyl units or additional solvent or matrix molecules. This explains why the presence of the trimethylsilyl groups in the position α to the coordinating nitrogen prevents the formation of the metal tetracarbonyl or metal pentacarbonyl species.

The TRIR experiments indicated that CO loss is a primary photoinduced process in cyclohexane solution at room temperature, but there is some indirect evidence for an η^6 to η^1 haptotropic shift of the pyridine ligand, i.e. the observation of (η^1-C_5H_5N)$Cr(CO)_5$, albeit in minor yield, following parent recovery. In the matrix experiments, η^6 to η^1 ring-slippage is clearly predominant over the loss of CO, which at first sight contrasts with the time-resolved IR spectroscopic observation in solution. However this apparent discrepancy is readily explained in terms of a very fast η^1 to η^6 haptrotropic reversal to the parent (reaction 4), which competes with

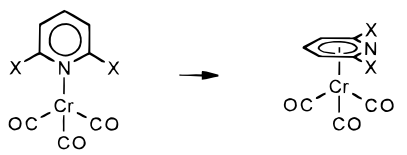

(4)

takeup of CO from solution resulting in the relatively low yield of (η^1-C_5H_5N)$Cr(CO)_5$.

The UV/vis experiments support this explanation. Monitoring the recovery of the depleted parent absorption at 340 nm, following pulse photolysis at 355 nm, demonstrated that this process follows a biphasic time profile (cf. inset in Figure 6). The faster of these two processes is completed within 40 ns, which is shorter than the rise-time of the TRIR equipment. We have assigned this portion of the recovery to the η^1 to η^6 haptotropic reversal (reaction 4). Thus, although the η^6 to η^1 ring-slippage process accounts for a significant proportion of the light absorbed by the complex, the ring-slippage product itself does not show up in the TRIR experiment. Moreover the yield of (η^1-C_5H_5N)-$Cr(CO)_5$ as a permanent photoproduct remains relatively low unless the η^1-species is trapped by a donor solvent such as methanol (Scheme 2). This accounts for the higher relative quantum yield for the conversion of (η^6-C_5H_5N)$Cr(CO)_3$ into (η^1-C_5H_5N)$Cr(CO)_5$ in CO-saturated CH_3OH compared to C_6H_{12}. The overall photochemical and subsequent thermal reactions of these compounds are summarized in Scheme 2.

Scheme 2[a]

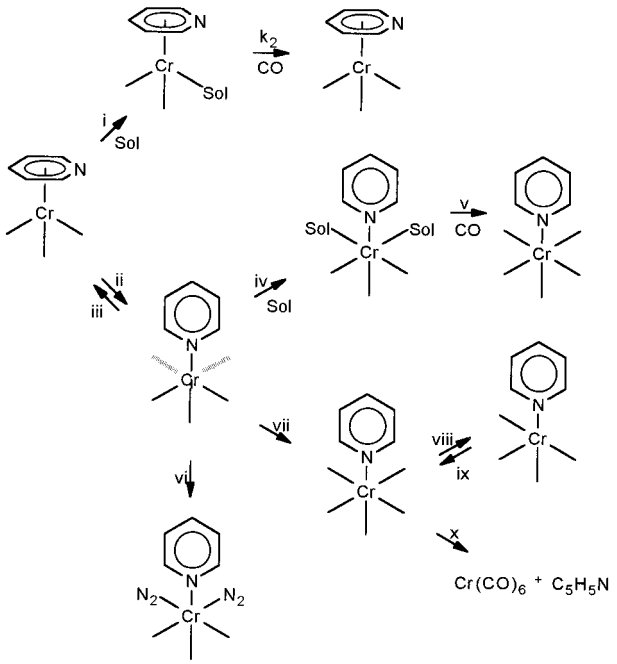

[a] CO ligands are represented as — for clarity. Reaction conditions: (i) λ_{exc} < 360 nm, Sol = cyclohexane (reaction 1); (ii) λ_{exc} > 308 nm; (iii) $\tau_{1/2}$ < 40 ns in cyclohexane (reaction 2); (iv) Sol = cyclohexane or methanol; (v) CO-saturated cyclohexane or methonol; (vi) λ_{exc} = 460 nm, N_2 matrix; (vii) λ_{exc} = 460 nm, 10% CO in CH_4 matrix; (viii) λ_{exc} = 250 nm, 10% CO in CH_4 matrix; (ix) λ_{exc} > 530 nm, 10% CO in CH_4 matrix; (x) $h\nu$, 10% CO in CH_4 matrix.

Concluding Remarks. It is apparent from this work that the application of a range of techniques is essential to fully appreciate the complexity of even a relatively simple system such as this. For instance the use of one technique, TRIR, would lead to an overly simplistic interpretation of the photochemical routes available. Furthermore these results demonstrate for the first time the importance of arene ring-slip processes in the photochemistry of (η^6-arene)$Cr(CO)_3$ compounds. The photochemistry of other (η^6-arene)$Cr(CO)_3$ systems

containing potential "traps" for ring-slip intermediates is currently under investigation.

Acknowledgment. The authors acknowledge the support of the European Union (HCM Programme, Contract No. CHRX-CT93-0152), The Irish American Partnership, and Forbairt (Ireland) (formerly Eolas) for support for G.R., M.T.P., and C.J.B., respectively. Professor R. N. Perutz and Professor M. Poliakoff are thanked for their helpful suggestions and comments. Dr. M. Viotte, G. Klihm, and D. Parirnus are thanked for their skilled technical assistance.

Supporting Information Available: Complete listings of bond lengths and angles, fractional coordinates, and thermal parameters and ORTEP diagrams for (η^6-2,6-$(CH_3)_2C_5H_3N$)-$Cr(CO)_3$ and (η^6-2,6-$((CH_3)_3)Si)_2C_5H_3N)Cr(CO)_3$ (12 pages). Ordering information is given on any current masthead page.

OM960090+